

# Creation, doubling and splitting of vortices in intracavity second harmonic generation

O-K Lim<sup>1</sup>, B Boland<sup>1</sup>, M Saffman<sup>1</sup> and W Krolikowski<sup>2</sup>

<sup>1</sup> Department of Physics, University of Wisconsin, 1150 University Avenue, Madison, WI 53706, USA

<sup>2</sup> Laser Physics Centre, Research School of Physical Sciences and Engineering, Australian National University, Canberra ACT 0200, Australia

Received 18 September 2003, accepted for publication 18 November 2003

Published 14 April 2004

Online at [stacks.iop.org/JOptA/6/486](http://stacks.iop.org/JOptA/6/486)

DOI: 10.1088/1464-4258/6/5/032

## Abstract

We demonstrate the generation and frequency doubling of unit charge vortices in a linear astigmatic resonator. The topological instability of the double charge harmonic vortices leads to well separated vortex cores that are shown to rotate, and become anisotropic, as the resonator is tuned across resonance.

**Keywords:** optical vortices, vortex splitting, second harmonic generation

Optical vortices are topological objects whose transformation properties under propagation in linear and nonlinear optical media have been the subject of much recent work [1]. The vortex charge of a beam, defined as the closed loop contour integral of the wave phase modulo  $2\pi$ , is generally a conserved quantity under linear propagation in free space. Optical vortices occur naturally in speckle fields [2], and can be generated in a controlled fashion using diffraction from holographic plates [3, 4]. They can also be generated in lasers [5–9] and cavities with nonlinear elements [10, 11], while high order vortex modes have been observed in active cavities with field rotating elements [12, 13]. Astigmatic optical elements as well as nonlinear wave interactions can be used to change the vortex charge of a beam. For example in the weak pump depletion regime of second harmonic generation the amplitude of the envelope of the harmonic field at frequency  $\omega_2$  can be written as  $A_2 \sim A_1^2$ . Thus an input field with charge  $m$  of the form  $A_1 \sim e^{im\phi}$  generates an output field  $A_2 \sim e^{i2m\phi}$  with twice the charge. This effect has been demonstrated experimentally by several groups using optical vortices created by diffraction from a hologram, and then allowing the beam to pass through a frequency doubling crystal [14–18].

In this work we describe a different approach to the generation of vortices in second harmonic generation that is based on frequency doubling of resonator modes with a vortical structure. Consider an empty resonator with the pump beam mode matched to the lowest order transverse resonator mode (TEM<sub>00</sub> mode), which has a slowly varying amplitude at the

cavity waist given by  $u_{00} \sim \exp(-r^2/w_c^2)$ , with  $\vec{r} = x\hat{x} + y\hat{y}$  and  $w_c$  the cavity waist. By changing the cavity tuning, and slightly tilting and displacing the pump beam, we can couple to higher order transverse modes of the cavity. By appropriate alignment of the pump beam it is possible to couple to a single higher order transverse mode, such as  $u_{10} \sim x \exp(-r^2/w_c^2)$  or  $u_{01} \sim y \exp(-r^2/w_c^2)$  which have edge dislocations. Following the cavity by an astigmatic mode-converter [19] the Hermite–Gauss modes can be efficiently converted into azimuthally symmetric Laguerre–Gauss modes with non-zero vortex charge, as was demonstrated by Snadden *et al* [20].

As we show here, it is also possible to generate a vortex mode directly, without using an astigmatic mode converter, by aligning the pump beam to give the desired superposition of  $u_{10}$  and  $u_{01}$  modes. Let the pump beam be a displaced and tilted Gaussian. Ignoring unimportant constant amplitudes, as well as any overall phase, we have  $u_p = \exp(-|\vec{r}-\vec{r}_p|^2/w_p^2) \exp(i\vec{q}\cdot\vec{r})$ . Here  $w_p$  is the pump beam waist,  $\vec{r}_p = x_p\hat{x} + y_p\hat{y}$  is the transverse displacement of the pump beam, and  $\vec{q} = q_x\hat{x} + q_y\hat{y}$  is the transverse wavevector that is proportional to the pump beam tilt in the  $x, y$  plane. The lowest order odd cavity mode that the pump couples to can be written as

$$u = o_{10}a(v - v_{10})u_{10} + o_{01}a(v - v_{01})u_{01} \quad (1)$$

where  $o_{mn} \sim \int dx dy u_p^* u_{mn}$  is an overlap integral, and  $a(v - v_{mn})$  is a complex coefficient that depends on the

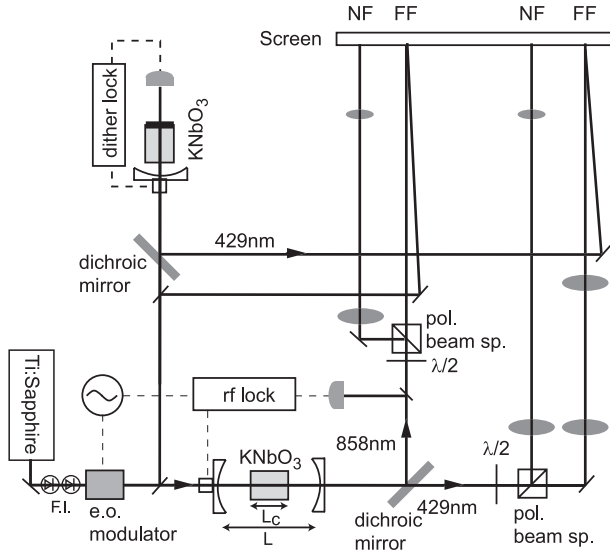


**Figure 1.** Experimental setup.

difference between the pump frequency  $\nu$  and the resonant frequency of the mode  $\nu_{mn}$ . The amplitude and phase of the overlap coefficients can be independently varied by adjusting the pump beam [21]. Performing the integrals we find  $o_{10} = h(2x_p/w_p - ik_x w_p)$  and  $o_{01} = h(2y_p/w_p - ik_y w_p)$ , where  $h$  is an unimportant common factor. By adjusting the pump beam we can obtain  $o_{01} = o_{10} \exp(i\pi/2)$  which results in vortex generation when  $a(\nu - \nu_{10}) = a(\nu - \nu_{01})$ .

Vortices were generated in this way using the experimental setup shown in figure 1. A Ti:sapphire laser at 858 nm generates a continuous wave fundamental beam with a power of up to 300 mW incident on the frequency doubling cavity. The beam is mode matched to a linear cavity with two  $R = 25$  mm end mirrors that contains a 1 cm long  $a$ -cut  $\text{KNbO}_3$  crystal with anti-reflection coated ends. The input and output mirrors had  $T_{858\text{nm}} = 4.8\%$ ,  $0.04\%$  and  $T_{429\text{nm}} = 92\%$  so that only the fundamental field was resonant in the cavity. Phase matching was controlled by varying the temperature of the crystal. With the distance between the mirrors set to  $L_{\text{cf}} = R + \frac{n_c - 1}{n_c} L_c = 30.7$  mm for confocal operation ( $n_c$ ,  $L_c$  are the crystal refractive index and length), and the crystal temperature tuned for large phase mismatch so no harmonic beam was generated, a cavity finesse of about 80 was measured. This agrees well with the theoretical value of  $F = 84$  that was calculated using measured values of the crystal losses. With the crystal temperature tuned for optimum phase matching up to about 60 mW of 429 nm light was generated in a  $\text{TEM}_{00}$  mode.

The cavity length was then reduced by 1.63 mm which resulted in the appearance of higher order transverse modes in the cavity transmission spectrum, as seen in figure 2. Using the measured free spectral range as a scaling parameter, the theoretically calculated frequencies of the first few higher order  $(q, m, n)$  modes have been indicated in the figure. The observed resonance frequencies agree to within a few per cent with the calculated values. The cavity was locked to a  $(q, 1, 0)$  resonance using the rf sideband technique [23] which resulted in stable generation of a unit charge vortex mode as seen in the inset of figure 2.

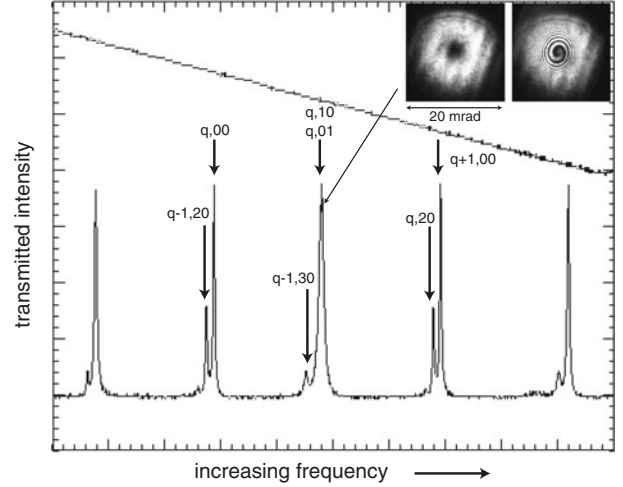


**Figure 2.** Scan of resonator transmission with theoretical positions of the modes marked by arrows.  $q$  denotes the axial mode index. The upper line is the linear ramp voltage applied to the cavity piezo, and the inset shows the far-field structure of the fundamental field at the odd mode resonance.

The phase structure of the harmonic field was observed by interference with a  $\text{TEM}_{00}$  beam generated in a second doubling cavity. As expected, the second harmonic beam contained a doubly charged vortex, as seen in figure 3. The detailed structure of the beam had a sensitive dependence on resonator alignment. Careful alignment of the crystal position resulted in observation of a doubly charged core region, although there was an apparent tendency for the vortices to repel each other so that a small vortex separation remained as seen in figure 3. We attribute the splitting to the topological instability of  $m > 1$  vortices [22]. Adjustments to the crystal and/or pump beam alignment resulted in the core splitting into two well separated singly charged vortices, with a controllable relative orientation and separation. It was also found that when the resonator was aligned so that the cores were well separated, the relative orientation angle of the cores rotated in a repeatable fashion as the resonator was tuned across the  $(q, 1, 0)$  resonance, as seen in figure 4.

The observations of vortex rotation can be explained by taking account of the cavity astigmatism due to crystal birefringence. Let the fundamental beam propagate along  $z$  ( $a$ -axis of  $\text{KNbO}_3$ ) and be polarized along  $y$  ( $b$ -axis). Beams propagating in the  $x$ - $z$  plane correspond to ordinary polarized rays with an index  $n_b = 2.279$  at 858 nm and the temperature set for phase matching. We will label the  $x$ - $z$  plane modes with the first transverse index  $m$  (the  $x$ -axis is horizontal in the figures). Beams propagating in the  $y$ - $z$  plane correspond to extraordinary polarized rays with an index  $n(\theta) = n_b(1 + \tan^2 \theta)^{1/2} / (1 + (n_b/n_a)^2 \tan^2 \theta)^{1/2}$  where  $\theta$  is the angle of the ray with respect to the  $y$  axis and  $n_a = 2.238$ . We will label the  $y$ - $z$  plane modes with the second transverse index  $n$ . The effective crystal thickness for  $x$ - $z$  plane modes is  $L_c/n_b$ , while the effective thickness for  $y$ - $z$  plane modes is  $L_c/\tilde{n}$ , where  $\tilde{n} = n_a^2/n_b$  is the effective index [24]. Since  $\tilde{n} < n_b$  the crystal is effectively longer in the  $y$ - $z$  plane and these modes have lower resonance frequencies. A short

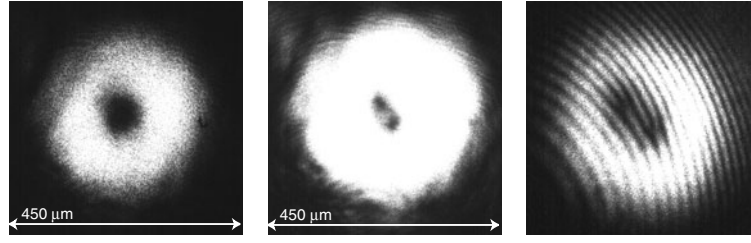


**Figure 3.** Near field images of the harmonic charge 2 vortex. The central frame is overexposed to reveal the vortex splitting, as verified by the far-field interferogram on the right.

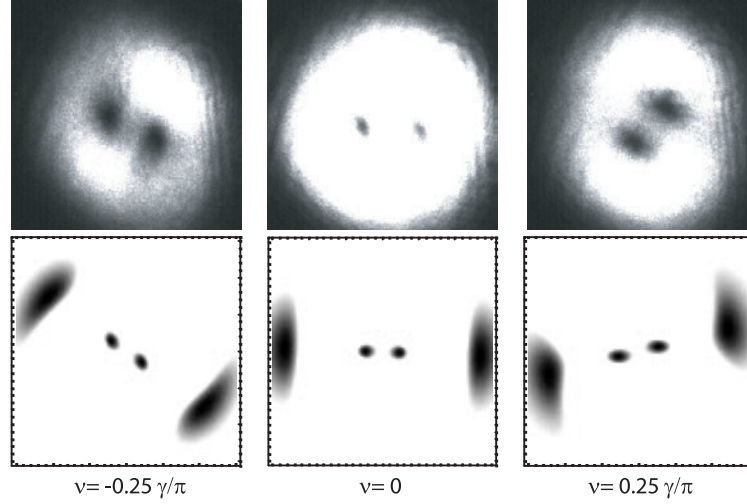


**Figure 4.** Rotation of harmonic vortices observed in far-field (top row) and calculated from equation (1) (bottom row). The columns are labelled with the pump beam frequency which increases from left to right.

calculation shows that the frequency splitting can be written as

$$v_{qm0} - v_{q0n} = \frac{c}{2\pi L_0} \left\{ (m+1) \cos^{-1} \left( \frac{\delta}{R} \right) - (n+1) \cos^{-1} \left[ \frac{\delta}{R} + \frac{L_c}{R} \left( \frac{1}{\tilde{n}} - \frac{1}{n_b} \right) \right] \right\} \quad (2)$$

where  $L_0 = R + [(n_c^2 - 1)/n_c]L_c + \delta$  with  $\delta = L - L_{cf}$  the change in cavity length from confocality. For our experimental parameters the shift given by equation (2) is about 15 MHz, which is a non-negligible fraction of the cavity resonance which has a FWHM of  $2\gamma = 2\pi \times 42$  MHz. Indeed, close inspection of figure 2 reveals that the odd order transverse modes are somewhat wider than the lowest order modes, in agreement with equation (2). The modal coefficient  $a$  that appears in equation (1) can be written as

$$a(v - v_{mn}) = [1 + (4F^2/\pi^2)^2 \sin^2(\pi(v - v_{mn})/(2\gamma F))]^{-1/2} e^{i \tan^{-1}(\chi_{mn})}, \quad (3)$$

where  $\chi_{mn} = f \sin[\pi(v - v_{mn})/(F\gamma)] / \{1 - f \cos[\pi(v - v_{mn})/(F\gamma)]\}$ , and  $f = 1 - \pi/F$ . For our experimental parameters the relative phase shift when the resonator is tuned to the midpoint between the (10) and (01) resonances is  $\tan^{-1} \chi_{10} - \tan^{-1} \chi_{01} \sim 40^\circ$ .

The simulations of vortex rotation shown in figure 4 were obtained by calculating  $u$  from equation (1), squaring the field, and adding a small constant offset which resulted in splitting of the vortices. The phase difference between  $o_{10}$  and  $o_{01}$  was set to  $\pi/2 - 40^\circ$  to give the correct  $\pi/2$  phase shift for  $v$  at the

midpoint between the modes, after which the frequency  $v$  was tuned across the resonance. We observe qualitative agreement between the observed rotation, and the calculated results. The reason for the calculated rotation being somewhat smaller than that observed may be that the calculations correspond to the near field while the observations shown in figure 4 were recorded in the far field. Additional observations revealed that the rotation angle was noticeably smaller in the near than in the far field. This is fully consistent with the propagation induced rotation of a vortex pair [14]. It should be emphasized however that the observed dependence of the rotation angle on the cavity tuning is not a propagation effect, but rather due to the interference of non-degenerate cavity modes with amplitudes given by equation (3). We also note that the shape of the vortex cores becomes elliptical on either side of the resonance. This may be due to the unequal changes in amplitude and phase of  $a$  which implies that we are generating and doubling anisotropic vortices [25].

In conclusion we have observed creation, doubling and splitting of vortices in a second harmonic generating resonator. Tuning of the resonator across a pair of non-degenerate transverse modes results in rotation of the harmonic vortex pattern.

## Acknowledgments

This work was supported by National Science Foundation grant 0200372. WK acknowledges support from the US Army Research Office and the Australian Research Council. MS is an AP Sloan Foundation fellow.

## References

- [1] Vasnetsov M and Staliunas K (ed) 1999 *Optical Vortices* (Commack: Nova Science)
- [2] Baranova N B, Zel'dovich B Ya, Mamaev A V, Pilipetskii N F and Shkunov V V 1981 *Pis. Zh. Eksp. Teor. Fiz.* **33** 206–10  
Baranova N B, Zel'dovich B Ya, Mamaev A V, Pilipetskii N F and Shkunov V V 1981 *JETP Lett.* **33** 195–9 (Engl. Transl.)
- [3] Bazhenov V Yu, Vasnetsov M V and Soskin M S 1990 *Pis. Zh. Eksp. Teor. Fiz.* **52** 1037–9  
Bazhenov V Yu, Vasnetsov M V and Soskin M S 1990 *JETP Lett.* **52** 429 (Engl. Transl.)
- [4] Heckenberg N R, McDuff R, Smith C P and White A G 1992 *Opt. Lett.* **17** 221–3
- [5] Rigrod W W 1963 *Appl. Phys. Lett.* **2** 51–3
- [6] Couillet P, Gil L and Rocca F 1989 *Opt. Commun.* **73** 403–8
- [7] Brambilla M, Battipede F, Lugiato L A, Penna V, Prati F, Tamm C and Weiss C O 1991 *Phys. Rev. A* **43** 5090–113
- [8] Brambilla M, Lugiato L A, Penna V, Prati F, Tamm C and Weiss C O 1991 *Phys. Rev. A* **43** 5114–20
- [9] Sleky G, Weiss C O, Tang D Y and Tarroja M F H 1994 *J. Opt. Soc. Am. B* **11** 2089–94
- [10] Arecchi F T, Giacomelli G, Ramazza P L and Residori S 1991 *Phys. Rev. Lett.* **67** 3749–52
- [11] Lippi G L, Ackemann T, Hoffer L M, Gahl A and Lange W 1993 *Phys. Rev. A* **48** R4043–6
- [12] Mamaev A V and Saffman M 1996 *Phys. Scr. T* **67** 21–5
- [13] Abramochkin E, Losevsky N and Volostnikov V 1997 *Opt. Commun.* **141** 59–64
- [14] Basistiy I V, Bazhenov V Y, Soskin M S and Vasnetsov M V 1993 *Opt. Commun.* **103** 422–8
- [15] Dholakia K, Simpson N B, Padgett M J and Allen L 1996 *Phys. Rev. A* **54** R3742–5
- [16] Beržanskis A, Matijošius A, Piskarskas A, Smilgevičius V and Stabinis A 1997 *Opt. Commun.* **140** 273–6
- [17] Beržanskis A, Matijošius A, Piskarskas A, Smilgevičius V and Stabinis A 1998 *Opt. Commun.* **150** 372–80
- [18] Torres J P, Soto-Crespo J M, Torner L and Petrov D V 1998 *Opt. Commun.* **149** 77–83
- [19] Tamm C and Weiss C O 1990 *J. Opt. Soc. Am. B* **7** 1034–8
- [20] Snadden M J, Bell A S, Clarke R B M, Riis E and McIntyre D H 1997 *J. Opt. Soc. Am. B* **14** 544–52
- [21] Anderson D Z 1984 *Appl. Opt.* **23** 2944–9
- [22] Mamaev A V, Saffman M and Zozulya A A 1997 *Phys. Rev. Lett.* **78** 2108–11
- [23] Drever R W P, Hall J L, Kowalski F V, Hough J, Ford G M, Munley A J and Ward H 1983 *Appl. Phys. B* **31** 97–105
- [24] Cheng Y-J, Fanning C G and Siegman A E 1997 *Appl. Opt.* **36** 1130–4
- [25] Molina-Terriza G, Wright E M and Torner L 2001 *Opt. Lett.* **26** 163–5